

The Lake Bosumtwi meteorite impact structure, Ghana— Where is the magnetic source?

Hernan UGALDE^{1*}, William A. MORRIS¹, Lauri J. PESONEN², and Sylvester K. DANUOR³

¹McMaster Applied Geophysics and Geological Imaging Consortium, School of Geography and Earth Sciences, McMaster University, 1280 Main Street West, Hamilton, Ontario, L8S 4K1, Canada

²Division of Geophysics, University of Helsinki, Helsinki, Finland

³Department of Physics, Kwame Nkrumah University of Science and Technology, Kumasi, Ghana

*Corresponding author. E-mail: ugaldeh@mcmaster.ca

(Received 25 July 2006; revision accepted 17 January 2007)

Abstract—The Bosumtwi impact structure (Ghana) is a young and well-preserved structure where a vast amount of information is available to constrain any geophysical model. Previous analysis of the airborne magnetic data and results of numerical simulation of impact predicted a strongly magnetic impact-melt body underneath the lake. Recent drilling through the structure did not penetrate such an expected impact-melt rock magnetic source. A new 3-D magnetic model for the structure was constructed based on a newly acquired higher-resolution marine magnetic data set, with consideration of the observed gravity data on the lake, previous seismic models, and the magnetic properties and lithology identified in the two International Continental Scientific Drilling Program (ICDP) deep boreholes. The new model contains highly magnetic bodies located in the northeast sector of the structure, not centered onto the drilling sites. As in previous models, higher magnetization than that measured in outcropping impactites had to be assigned to the unexposed source bodies. Integration of the new model with the borehole petrophysics and published geology indicates that these bodies likely correspond to an extension to the south of the Kumasi batholith, which outcrops to the northeast of the structure. The possibility that these source bodies are related to the seismically identified central uplift or to an unmapped impact-melt sheet predicted by previous models of the structure is not supported. Detailed magnetic scanning of the Kumasi batholith to the north, and the Bansu intrusion to the south, would provide a test for this interpretation.

INTRODUCTION

Impact cratering processes are essential for the understanding of the geological and biological evolution of planet Earth. Terrestrial impact cratering research is important as the Earth is the only planet from which we can obtain a reasonable spatial and temporal impact record. Integration of results from seismic surveys, potential field studies, remote sensing, drilling, and numerical modeling of impact processes, coupled with petrophysical data of impactites and target rocks, provides constraints on determining crater dimensions and processes involved in crater formation (Artemieva et al. 2004). Analysis of gravity and magnetic data of ancient impact structures gives estimates for the degree of the erosion, and thus provides a tool for estimating the original dimensions of deeply eroded structures (Pilkington and Grieve 1992; Plado et al. 2000; Ugalde 2006). Such data may also be crucial to delineate

impact breccia, especially the often strongly magnetic impact melt bodies.

The Bosumtwi impact structure in Ghana (6°30'N, 1°25'W) is a unique terrestrial case that allows us to study how an impact structure on Earth has been formed. The structure is located about 30 km southeast of Kumasi (Fig. 1). The crater is occupied by Lake Bosumtwi and has a rim-to-rim diameter of 10.5 km (Koeberl and Reimold 2005). The lake itself has a diameter of 8 km and a maximum depth of 75 m (Scholz et al. 2002). The crater structure is the youngest of the moderately large and well-preserved impact structures on Earth; the Bosumtwi impact structure was formed by a meteorite impact about 1.07 Myr ago in lower greenschist facies supracrustal rocks of the 2.1–2.2 Gyr old Birimian Supergroup, which are intruded by various mostly granitic and granodioritic bodies (Koeberl et al. 1997; Koeberl and Reimold 2005) (Fig. 2). Based on recent numerical modeling and tektite distribution analysis, the Bosumtwi crater was

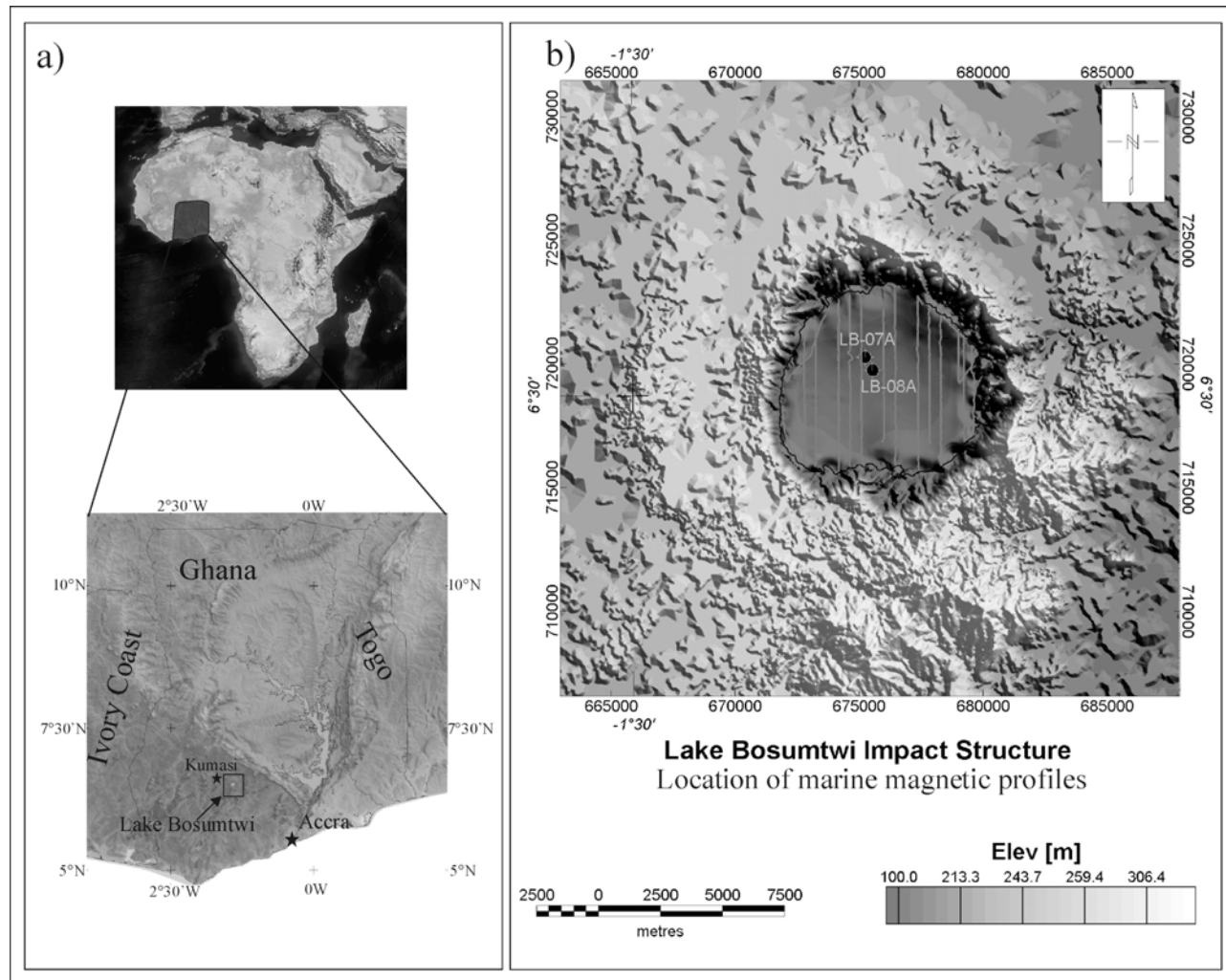


Fig. 1. a) The location of Lake Bosumtwi in Africa (top) and Ghana (bottom). The bottom panel shows topography data from SRTM. The cities of Accra and Kumasi are marked for reference. The rectangle in the bottom panel marks the location of the detailed image on the right. b) The topography of the lake area and location the marine magnetic profiles. The positions of the 2004 ICDP deep boreholes are shown for reference.

likely produced by an iron meteorite which came probably from the northeast with a velocity of $\sim 20 \text{ km s}^{-1}$ and impacted the Birimian target rocks at an angle of $30\text{--}45^\circ$ (Artemieva et al. 2004).

The structure is accessible and a wide variety of geophysical (airborne, shipborne) data has been accumulated to allow detailed geophysical modeling. In addition, a recent International Continental Scientific Drilling Program (ICDP) drilling project into Lake Bosumtwi in 2004 (Koeberl et al. 2007; Coney et al. 2007; Ferrière et al. 2007) has provided significant new ground truth with which to calibrate the geophysical data sets for the interior of the structure. Based on a high-resolution airborne magnetic survey and then available petrophysical and paleomagnetic data, Plado et al. (2000) presented a magnetic model for the Bosumtwi structure. The model suggests the presence of a highly magnetic impact-melt body just north of the lake center. In order to reproduce the observed magnetic anomalies, the

magnetic parameters of the model (susceptibility and intensity of remanent magnetization) had to be much higher than those of suevites accessible in outcrop to the north and south of the lake (for a review of the geology, see Koeberl and Reimold 2005). The model was constructed from polygonal prisms located between 200 and 600 m depth. The Plado et al. (2000) model was subsequently shown to be consistent with numerical models of the cratering process and the related estimate of impact-melt production estimation (Artemieva et al. 2004).

Since 2000, seismic and gravity surveys have been carried out across Lake Bosumtwi (Karp et al. 2002; Scholz et al. 2002). The results of the seismic surveys point to a four-layer structure consisting of water, sediments, impact breccia, and unfractured basement at the bottom. In this modeling, the breccia layer resembled the magnetic melt body of Plado et al. (2000). The seismic data outlined a double-peaked central uplift below the lake sediments. The location of the central

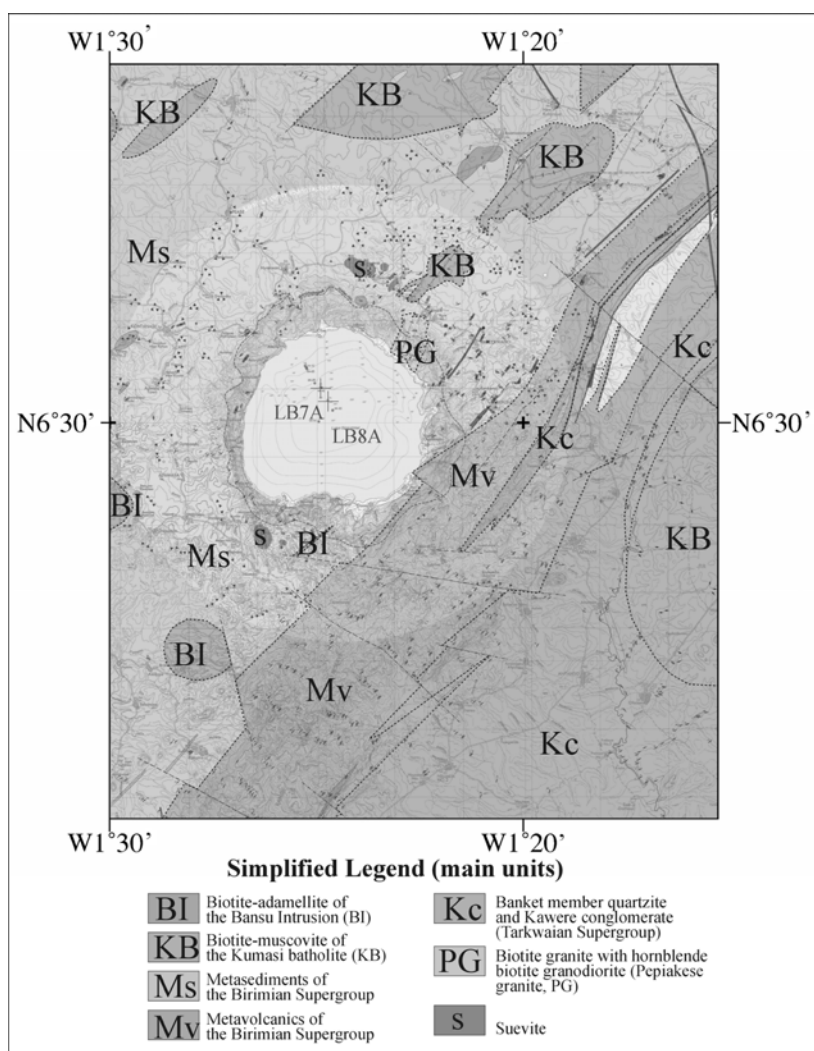


Fig. 2. A simplified geological map of the Bosumtwi impact crater area (modified after Koeberl and Reimold 2005).

uplift is slightly to the northwest of the center of the crater structure. A gravity-based 3-D model supports the water-sediment-breccia structure and is consistent with sediment thickness and geometry of the central uplift as indicated by the seismic data. However, this gravity model is unable to locate the breccia-basement interface because of a lack of a sufficient density contrast between the two units (Ugalde et al. 2007).

The two deep boreholes through the interior of the structure (LB-07A, LB-08A) revealed some surprises. Although the drilling yielded unequivocal evidence of the three anticipated upper layers (Coney et al. 2007; Ferrière et al. 2007), it did not penetrate the hypothesized highly magnetic body in the structure. Instead, drilling went through a weakly magnetic breccia with only minor amounts of impact-melt fragments (Coney et al. 2007; Ferrière et al. 2007; Elbra et al. 2007; Kontny et al. 2007; Morris et al. 2007). The borehole magnetic logging revealed distinct short-wavelength magnetic anomalies in the bottom part (Morris

et al. 2007). However, those anomalies must be analyzed carefully, as they were determined from samples spaced at 10 cm intervals and with a millimeter-scale source-sensor separation. Therefore, the amplitude and frequency components of these anomalies are not directly comparable to the marine and airborne magnetic data sets. Petrophysical scanning of the cores is generally consistent with the borehole logs and shows sporadic susceptibility and remanence enhancements (Elbra et al. 2007; Kontny et al. 2007; Morris et al. 2007). However, these susceptibility values are one order of magnitude lower than the values required by the Plado et al. (2000) model. The questions therefore are: where is the magnetic source body and how was it formed? What rock type is causing the anomalies? Are the borehole anomalies related to the hidden magnetic body or are they related to more local layers within the stratigraphy?

To answer these questions we re-analyzed the airborne and marine magnetic data for the Bosumtwi structure. The goal was to obtain a new magnetic model which would be

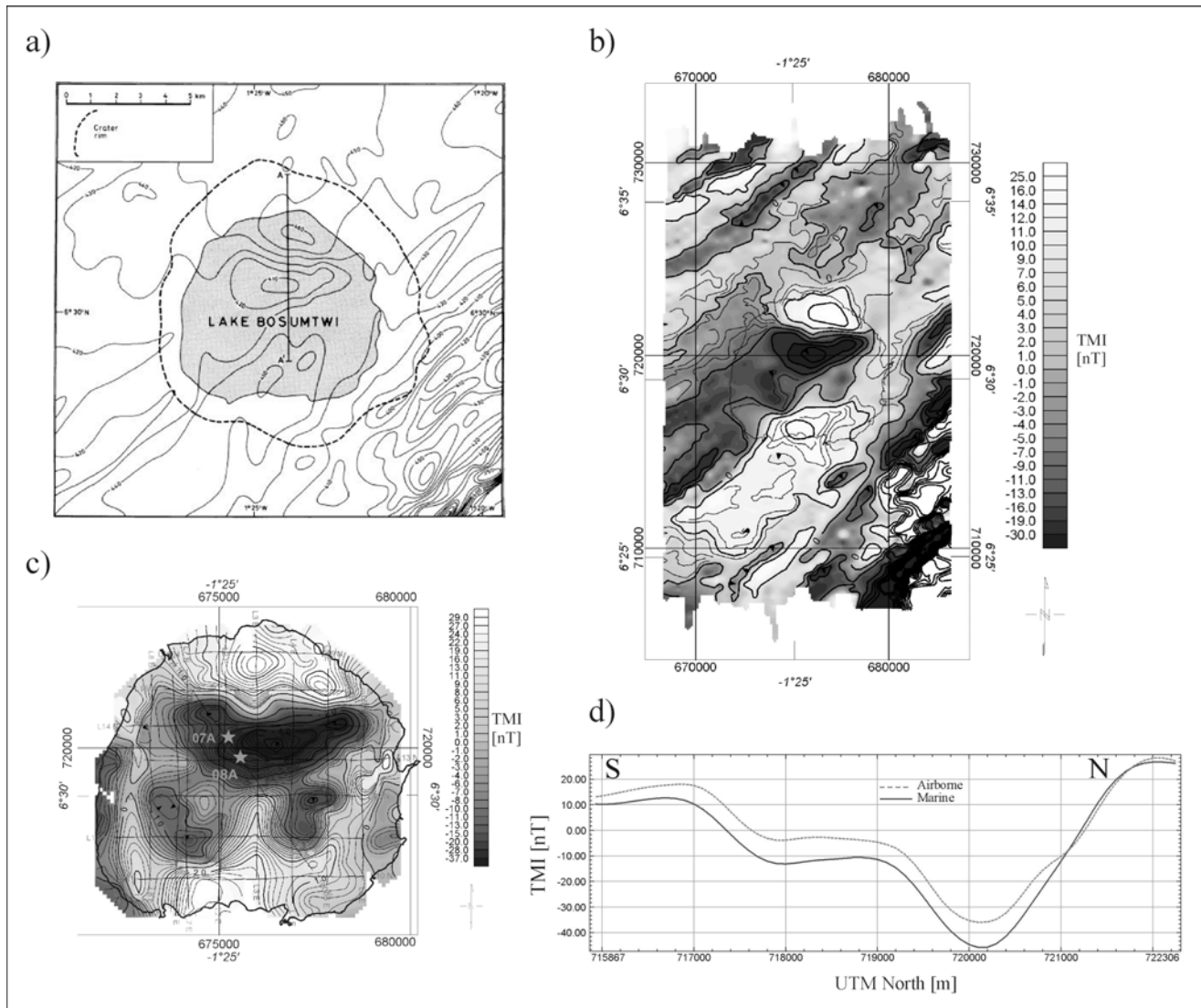


Fig. 3. The total magnetic field at Lake Bosumtwi. a) The 1960 airborne survey, as published by Jones et al. (1981). b) The 1997 airborne residual anomaly map, after Plado et al. (2000). Data from Pesonen et al. (2003). Contour interval is 2 nT. c) The 2001 marine survey. The data collection lines are noted in black, and the location of the 2004 ICDP drilling sites are marked as stars. The lake outline is in black. The contour interval is 2 nT. Data from Danuor (2004). d) A south-north profile across the structure (line 4E of [c]), showing both the marine (lake level) and airborne (70 m altitude) data sets for comparison. Note the greater amplitude of the marine data, due to its location closer to the magnetic sources.

consistent with existing petrophysical and paleomagnetic data sets (Elbra et al. 2007; Kontny et al. 2007; Schleifer et al. 2006) as well as the gravity and seismic data.

THE BOSUMTWI IMPACT STRUCTURE

Regional Geology

The regional Precambrian geology in and around Lake Bosumtwi is dominated by the 2.2–2.1 Gyr old supracrustal rocks of the Birimian Supergroup, comprising mainly meta-graywackes, shales, and mica schists, and occurring in the form of several broad metasedimentary and metavolcanics

belts (Karikari et al. 2007). A characteristic feature of the supracrustal rocks is a northeast-southwest fabric trend with steep dips either to the northwest or southeast (Reimold et al. 1998) (Fig. 2). These regional belts are easily recognized in aeromagnetic maps (Fig. 3b). A variety of granitoid intrusions (biotite or amphibole granites) is also present in the Bosumtwi region (Junner 1937; Moon and Mason 1967; Koeberl and Reimold 2005). Granite intrusions, probably connected with the Kumasi batholith, outcrop around the north, northeast, east, and west sides of the lake, (e.g., the Pekiakese granite on the northeast side of the lake [Jones et al. 1981; Koeberl and Reimold 2005]). Biotite and hornblende granodiorites (Bansu intrusion) (Koeberl and Reimold 2005)

outcrop to the south and west of the lake. Numerous narrow dikes of biotite granitoid occur at many basement exposures in the crater rim (Reimold et al. 1998).

Recent rock formations include the lake beds and the products of weathering (laterites, soil) which can have thicknesses up to 10 m. Although no impact melt rock has been found around the crater (Jones et al. 1981; Reimold et al. 1998), numerous breccia and suevite exposures have been mapped (Koeberl and Reimold 2005). In early 1999, a shallow drilling program to the north of the crater rim was undertaken to determine the extent of the ejecta blanket around the crater and to obtain subsurface core samples for mineralogical, petrological, and geochemical studies of ejecta (Boamah and Koeberl 2003). A variety of impactite breccias were found, including impact glass-rich suevite and several types of lithic breccias (Boamah and Koeberl 2003).

The impact origin of the structure was proven, e.g., by evidence of shock deformation features (e.g., planar deformation features [PDFs], high pressure mineral phases in impactites). For a review, see Koeberl and Reimold (2005) and references therein.

PREVIOUS GEOPHYSICAL STUDIES

Magnetic Data

The first airborne magnetic study of the structure was made in 1960 by Hunting Surveys Ltd. (Jones et al. 1981) at a flight altitude of 300 m and with a line spacing of 500 m. The occurrence of a central negative magnetic anomaly of ~40 nT, with positive side (flank) anomalies of ~20 nT was reported (Fig. 3a). The anomaly was modeled with a 200 m thick breccia lens below the lake sediments occurring at a depth of 500 m.

In 1997, a high-resolution low-altitude (70 m) airborne geophysical survey across the Bosumtwi structure was carried out by the Geological Survey of Finland in cooperation with the University of Vienna and the Ghana Geological Survey Department (Pesonen et al. 1997; Pesonen et al. 2003). It included measurements of the total magnetic field, electromagnetic field, and gamma radiation data. Line spacing was 500 m and the sampling rate 7.5 m (magnetics), 15 m (EM), and 60 m (radiometric), respectively, along north-south flight lines (Pesonen et al. 2003). A series of 21 geophysical maps (magnetic, electromagnetic, radiometric) of the structure were compiled by these authors.

After eliminating the regional magnetic field, Plado et al. (2000) published a residual magnetic anomaly map of the Bosumtwi structure which is strikingly similar to the one published by Jones et al. (1981) but much more detailed (Fig. 3b). The central part of the structure is characterized by relatively high gradients. At the center of the lake there is one large negative magnetic anomaly with two positive side anomalies to the north and south of it, consistent with the

expected expression of a magnetic source at near-equatorial magnetic latitudes (see Fig. 5 of Pesonen et al. 2003).

Investigation of the magnetic anomaly pattern (Fig. 3b) clearly illustrates the idea that the impact occurred into a southwest-northeast trending metasedimentary-metavolcanic belt. This belt is not as strongly visible at the lake as is the similarly trending (southwest-northeast) belt to the southeast side of the structure, which is superimposed by the impact structure at its southwest edge. There is a weak ring-shaped magnetic halo around the lake. The central negative anomaly is oblique to the overall southwest-northeast trending magnetic lineation, and it is seemingly composed of 4 to 6 patches. It is flanked by northerly and somewhat weaker southerly positive anomalies. A weakly positive anomaly spot almost at the center of the lake was interpreted by Plado et al. (2000) as a possible central uplift.

In 2001, the Kwame Nkrumah University of Science and Technology (KNUST, Kumasi, Ghana) collected a marine magnetic data set to complement the existing airborne data (Danuor 2004). This new data set had a wider spacing of 800 m, and the magnetometer was towed behind the marine platform used for that purpose. Albeit having a wider line spacing than the airborne data set, the marine data had the advantage that it measured the magnetic field closer to the magnetic sources. Also because of the slower movement of the platform, the sampling rate was improved. The smaller distance to the sources and enhanced sampling rate allows a better representation of the magnetic anomalies, which can not be achieved by pure downward analytical continuation from the airplane data collection surface to the lake level. Figure 3d shows a south-north profile across the main part of the magnetic anomaly with both the marine and airborne magnetic data sets. The greater amplitude of the marine data set can be observed. In order to isolate the main magnetic anomalies and their probable causative bodies, we computed the amplitude of the analytical signal, which is computed as $ASIG(X, Y) = \sqrt{(\partial F/\partial X)^2 + (\partial F/\partial Y)^2 + (\partial F/\partial Z)^2}$ (Nabighian 1972) and gives maxima over the edge of the magnetized bodies causing the observed anomalies, with the advantage of being independent of remanent magnetization (Nabighian 1972; Roest et al. 1992; MacLeod et al. 1993). The NE of the lake exhibits a couple of high-amplitude, mid- to long-wavelength anomalies (A1, B1 of Fig. 4). There is a large anomaly that encircles the northern part of the lake, which previously had been tentatively interpreted as a large package of highly magnetic melt-rich rocks. However, the analytical signal map of Fig. 4 permits the separation of the anomaly into at least three main high-amplitude anomalies of about 1000–2000 m wavelength (see Fig. 4, anomalies A1, A2, A3), plus some highly magnetized material to its sides. The rest of the lake does not exhibit any other significant anomalies, except for the previously noted B1, and anomalies B3 and B2 (composed of two smaller magnetic sources) to the south of it. B1 and B2 are aligned in a SW-NE trend, parallel

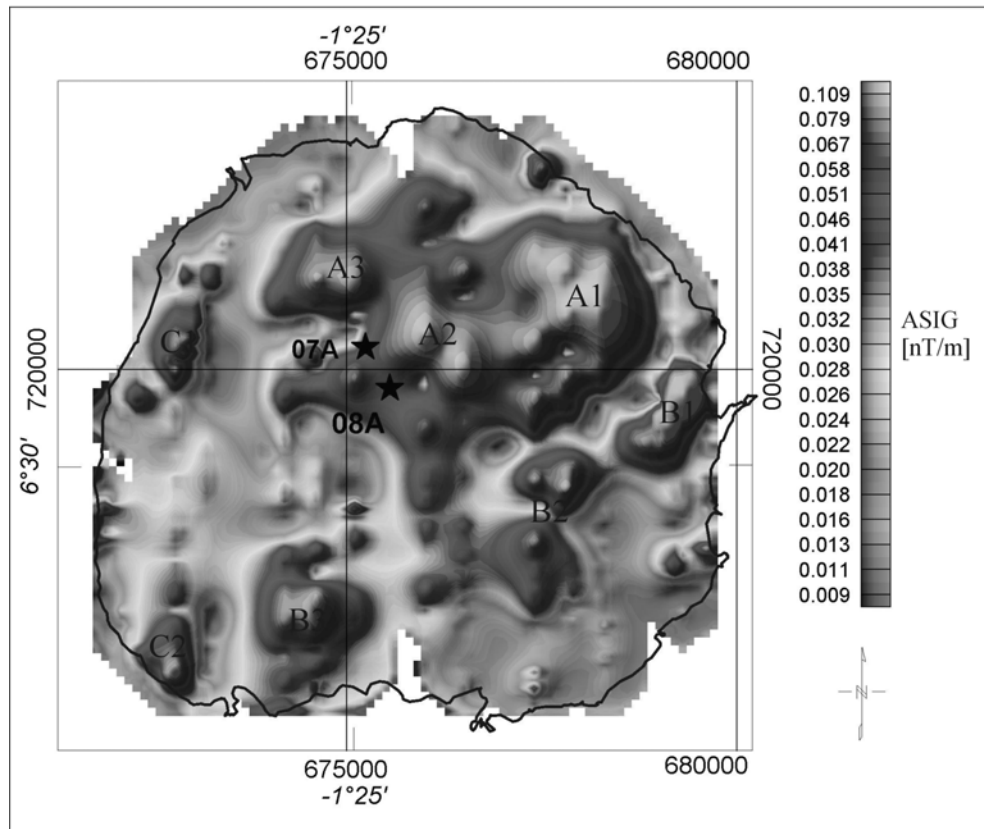


Fig. 4. Amplitude of the analytical signal (ASIG), computed from the marine magnetic data set. The two ICDP deep boreholes are shown as stars. The main anomalies are labeled. See text for details.

to the dominant strike of the metasedimentary and metavolcanic belts observed in the region; and anomalies C1 and C2, at the western side of the lake, both have mid- to high- amplitude and 700–900 m wavelength. The smaller amplitude of C1 and C2 denotes probable deeper settings of their corresponding magnetic sources, or poorer magnetic properties than those relating to the anomalies A and B.

Magnetic Properties of the Rocks

The magnetic properties of the rocks found in and around the Bosumtwi structure are of key importance in the modeling. The data used by Plado et al. (2000) are summarized in Table 1 together with data used in this work.

Plado et al. (2000) demonstrated that there is a clear difference between petrophysical properties of the target rocks and the impact-derived suevites. The fallout suevites have lower densities (higher porosities) and somewhat higher magnetizations (susceptibility, remanent magnetization) compared to the target rocks. The remanent magnetization of suevites prevails over induced magnetization (the Koenigsberger ratio of remanent over induced magnetization is much higher than 1: $Q = \frac{\|\overline{M}_R\|}{\|\overline{M}_I\|} \sim 4$). The target rocks have strikingly homogeneous physical properties with noticeable weak remanent magnetization and Q values

($Q < 0.05$). A graphitic shale had fairly high remanent magnetization (natural remanent magnetization [NRM] = 3.86 A/m, $Q = 0.67$), whereas the granites (such as the Pekiakese body) were magnetically very weak (NRM < 0.2 A/m, $Q < 0.16$). Unfortunately, there are no measurements of magnetic properties for the Kumasi batholith to the north of the lake and the Bansu intrusion to the south, although both of them exhibit a direct spatial correlation with the airborne magnetic anomalies.

Petrophysical measurements were accomplished on the core recovered from both holes LB-07A and LB-08A at the facilities of the GeoForschungsZentrum (GFZ) in Potsdam in 2004 (Milkereit et al. 2006; Ugalde 2006; Morris et al. 2007). See Morris et al. (2007) for a detailed description of the magnetic susceptibility logging.

NRM was measured in a few selected samples of the cores (Elbra et al. 2007; Kontny et al. 2007). In general, NRM intensities on impact breccias vary between 0.4 and 20 A/m (Kontny et al. 2007). Although these values are higher than the NRM intensities reported for the target rocks sampled around the lake (0.1–39 mA/m) (Plado et al. 2000), they were derived from small clasts or pieces of melt, and therefore do not constitute a representative high-magnetization unit that could account for the large magnetic anomalies observed in the lake area.

Table 1. Magnetic properties of the impact and target rocks as measured on outcrops around Lake Bosumtwi by Plado et al. (2000) and on the LB-07A and LB-08A drill cores (Kontny et al. 2007), and magnetization parameters used in the 3-D model.

Rock type/layer	Magnetic susceptibility Plado et al. (2000)		Magnetic susceptibility This work		Remanent magnetization Plado et al. (2000) (A/m)		Remanent magnetization This work (A/m)	
	Measured	Model	Measured	Model	Measured	Model	Measured	Model
	Water	N. A.	N. App.	N. A.	0	N. A.	0	N. A.
Sediments	N. A.	N. App.	N. A.	0	N. A.	0	N. A.	0
Magnetic bodies	0.00033	0.0033	0.0003	0.0002–0.05	0.0368	0.0368 $D = 3$ $I = -1$	0.0004–0.2	0–15 $D = -6$ $I = -12$
Target rocks (background)	0.00015	0	0.0003	0.0003			0.057	0

N. A. = not available; N. App. = not applicable.

Previous Magnetic Models

Based on aeromagnetic data and petrophysical and paleomagnetic data of oriented samples of impactites and target rocks outcropping around the lake, Plado et al. (2000) published a 3-D magnetic model of the structure. The model consisted of polygonal bodies at depth from 200 to 600 m diminishing downwards from their surface cross section. The model of Plado et al. (2000) is shown in Fig. 5a.

However, in order to obtain a meaningful match of the model with the observed magnetic data, Plado et al. (2000) had to assign much higher values to the magnetic properties to the body than what was actually measured on rocks (see Table 1). In the model, water, sediment, and basement were all treated as the same background unit with zero magnetization. The magnetic body constituting the source of the magnetic anomaly (the hypothesized impact melt) was given uniform magnetic properties (susceptibility = 0.0033 SI, NRM = 0.367 Am^{-1} and $Q \sim 4.3$). The remanent magnetization direction was set to $D = 3$, $I = -1$, as measured on suevites outcropping around the lake. Plado et al. (2000) discussed in detail the various possibilities for why the magnetic parameters within the structure could differ from those outside.

Danuor obtained a 2.5-D model for one profile across the center of the structure (Danuor 2004). Similar to Plado et al. (2000), in order to reproduce the observed anomaly, he used a high magnetic susceptibility of 0.03 SI, but assumed only induced magnetization (no NRM). The proposed source body extended from about 250 m to about 610 m depth (Danuor 2004). Danuor's model is shown in Fig. 5b.

NEW MAGNETIC MODELING

Synthetic Modeling

Due to the dipolar nature of the Earth's magnetic field, observed magnetic anomalies at low magnetic latitudes can be rather complex, and thus to find the proper location of the magnetic sources relative to the anomalies can be difficult. To better understand the expected pattern of magnetic anomalies

at low magnetic latitudes as at Lake Bosumtwi, we first performed some synthetic modeling.

The first model (Figs. 6a–c) shows the magnetic signature of a magnetized prismatic body of $4000 \times 4000 \times 400$ m. The size of the body is the same as that assumed by Plado et al. (2000). This proves that a highly magnetic anomalous source body will give rise to a negative magnetic anomaly at the observed latitude (6.5°N) of Lake Bosumtwi. The negative anomaly appears slightly to the south of the center of the body and is accompanied by positive anomalies on the northern and southern sides of the major anomaly. Of these side anomalies, the northern one has slightly higher amplitude than the southern one. From this model, it is also clear that the measured magnetization parameters of the deep ICDP boreholes LB-07A and LB-08A are insufficient to generate the observed magnetic anomaly. Adding remanent magnetization parallel to the ambient field has the same effect as increasing the magnetic susceptibility: the shape of the anomaly does not change, only its amplitude.

The second synthetic model (Fig. 6d) shows the magnetic signature of a thin sheet of $4000 \times 4000 \times 5$ m. The purpose of this model is to test the hypothesis of the observed magnetic anomaly being caused by a stack of thin melt sheets. This hypothesis arose at early stages of interpretation of the LB-07A and LB-08A borehole magnetic data, which showed high-frequency and high-amplitude magnetic anomalies. However, the borehole data were acquired at a sampling rate of 10 cm and spacing of millimeters between the magnetic sources and the sensors therefore, the frequency content of these anomalies is related to the different sampling rate and closer distance to the magnetic sources, and is not comparable to the observed magnetic anomalies as detected from the lake surface or from an airplane. In any case, this model is intended to verify whether the thin magnetic sheet idea is feasible or not. The magnetization parameters used are the same as for the 3-D model (Table 1). The amplitude of the anomaly created by such a thin sheet is 0.25 nT at a depth of 200 m, and 0.04 nT at 600 m depth. Thus, to reproduce the observed ± 30 nT anomaly, we need at least 120 of these thin sheets, assuming the best possible scenario of shallow sources at 200 m where the amplitude is the greatest. If we

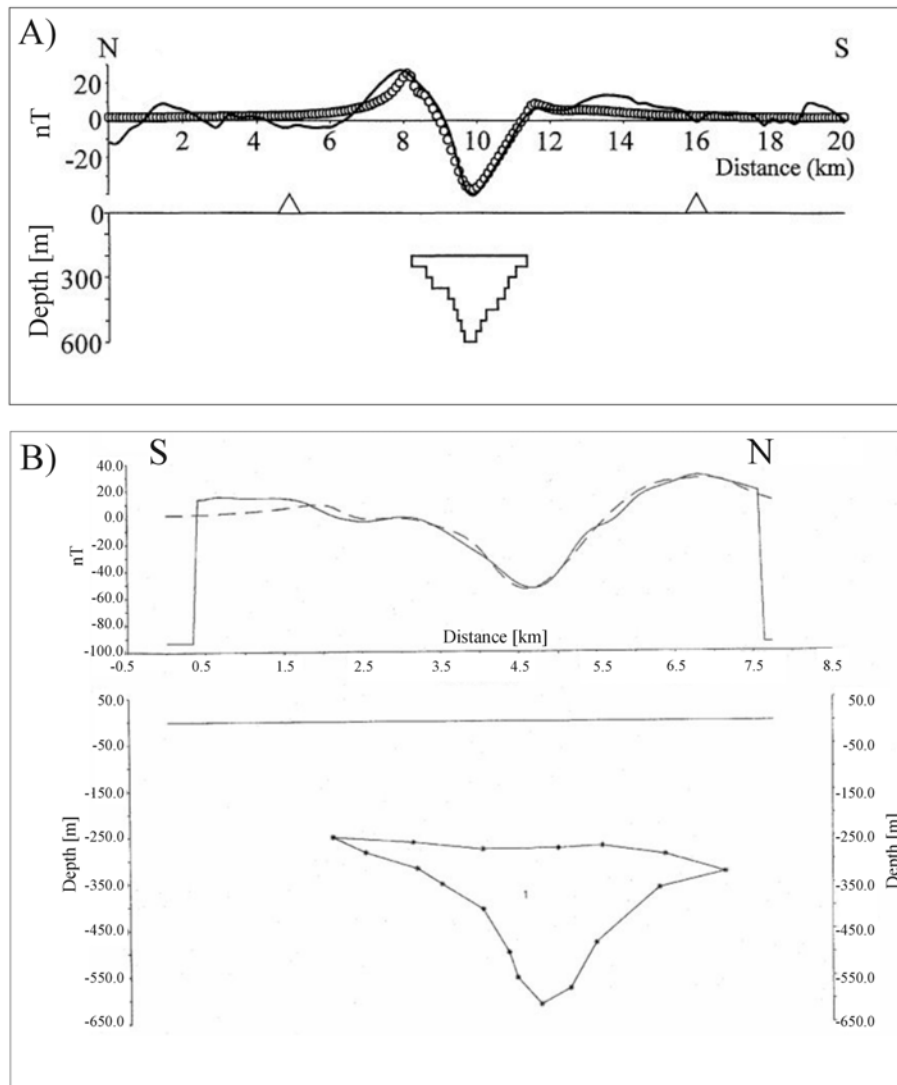


Fig. 5. Previous attempts to model the observed magnetic anomalies at Lake Bosumtwi. a) A cross section through the center of the crater, from Plado et al. (2000). b) The Danuor (2004) model across the center of the structure. Note the different directions and scales for these two profiles.

consider the decreasing amplitude with depth, the number of sheets scales up to at least 200. Therefore, the more realistic approach of stacking the thin sheets one below the other, leaving some space in between them, would first require more space (>1000 m, taking into account 1000 m for the 200 thin sheets, plus 60–100 m of host rock considering 0.5–1 m between each sheet), and secondly the computed magnetic response of such a geometry would still be smaller than the observed field. Furthermore, this alternate model would extend from 200 to 1200 m depth, which is not feasible according to the borehole logs (Coney et al. 2007; Deutsch et al. 2007; Ferrière et al. 2007), and also would mean a block of $4000 \times 4000 \times 1000$ m of highly magnetic material, which was not encountered by the deep ICDP boreholes.

New 3-D Model

A new 3-D model was created from the marine magnetic data (Fig. 7). The 3-D structure was built over the ~ 800 m spaced north-south profiles. Each section is 850–1000 m wide (depending on the separation of the survey lines). The bodies that constitute each section are draped over the crater bathymetry. A combination of forward modeling and inversion leads to a model that has an error with an average of 0.84 nT and a standard deviation of 8.2 nT. The basic model, which was constructed on the basis of the geometry inherited by a similar 3-D model built with the gravity data (Ugalde et al. 2007), comprises four layers: water, sediment, impact breccia (or magnetic rocks underlying the sediments), and—for consistency with Kontny et al.'s (2007) petrophysical

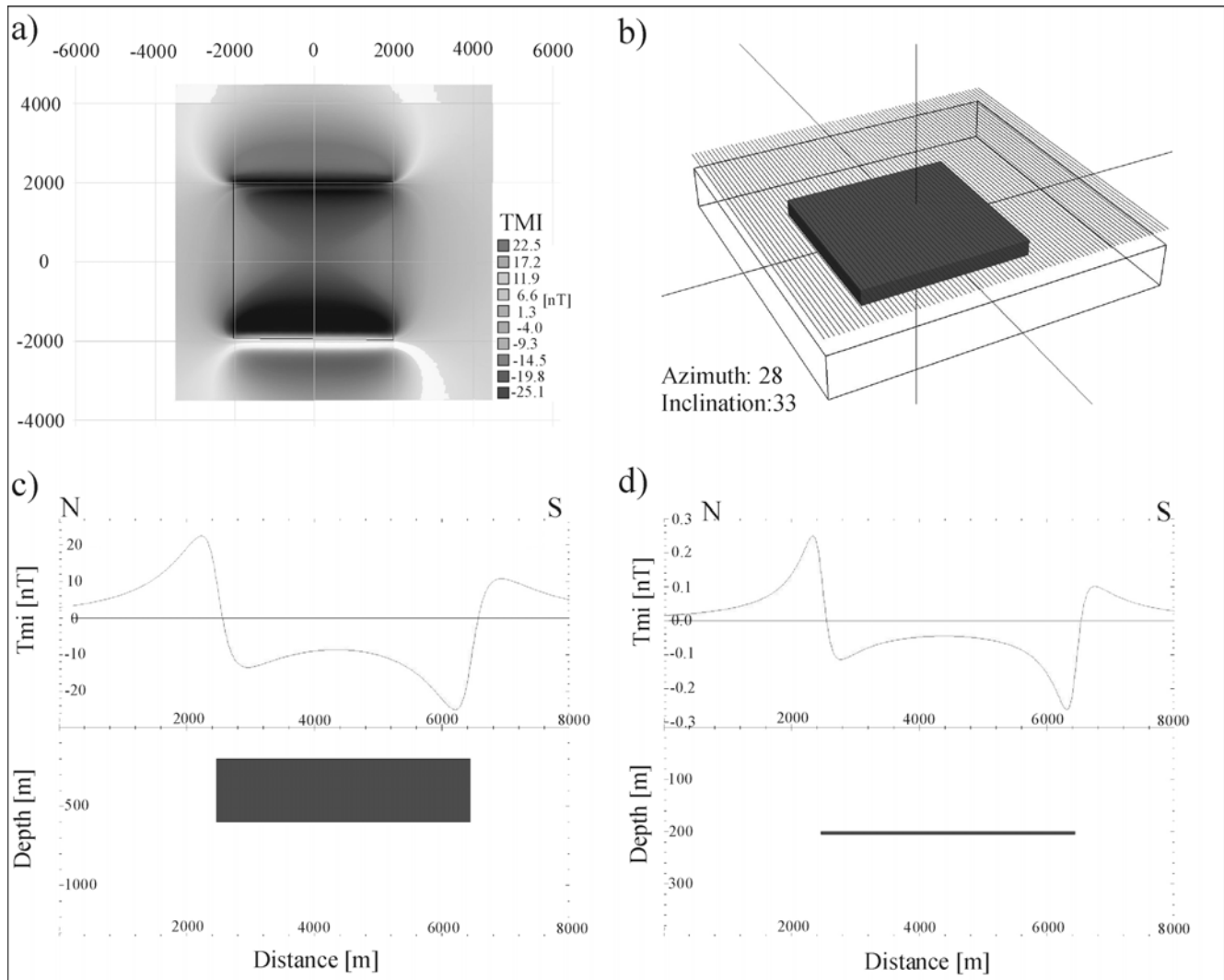


Fig. 6. Synthetic models for a source at a magnetic latitude similar to that of the Lake Bosumtwi impact structure. The magnetic source is one magnetized block, with the parameters as given in Plado et al. (2000). See text and Table 1 for details. a) Plan view of the model (black outline) and its computed magnetic response. b) 3-D perspective view of the model, showing the synthetic lines every 100 m. c) Cross section of the model along the center of the synthetic structure. d) Cross section of the thin sheet model. Note the different vertical scales in (c) and (d).

measurements—a magnetic background. Kontny et al. (2007) measured high remanent magnetization intensities on samples from both ICDP deep boreholes (LB-07A and LB-08A), which vary depending on the volume percent content of pyrrhotite. However, those magnetization variations on the background are beyond the resolution of the marine magnetic data set used here.

The parameters used in this model calculation are summarized in Table 1. Starting from the source body geometry derived from the gravity study and applying inversion, the magnetic properties of the bodies constituting each line were adjusted line by line in order to reproduce the observed anomalies. The inversion was constrained to magnetic susceptibilities <0.05 SI and NRM <15 A/m. What makes this model really 3-D is that all the bodies across the entire structure are active when computing a single line, thus

unlike 2-D or 2.5-D models, each line is affected by the bodies located laterally to it. As seen in Fig. 7, this model allows a non-uniform magnetization distribution throughout the structure. Magnetic susceptibilities vary from 0.0002 to 0.05 SI and NRM intensity from 0 to 15 A/m, parallel to the ambient field ($D = -6^\circ$, $I = -12^\circ$).

The model complies to the borehole petrophysics, with magnetic susceptibilities and remanence values within the range of what was measured on the recovered core from the deep ICDP boreholes (Elbra et al. 2007; Kontny et al. 2007; Morris et al. 2007). The susceptibility values are uniformly low across most of the lake, with the exception of the northeast side of it. There, at a distance of ~ 1800 m from the ICDP boreholes lie 4 bodies that cover an area of $\sim 4000 \times 2000$ m and where susceptibilities are much higher than those measured on the IDCP core (Fig. 7) (Figs. 3 and 4 of Morris

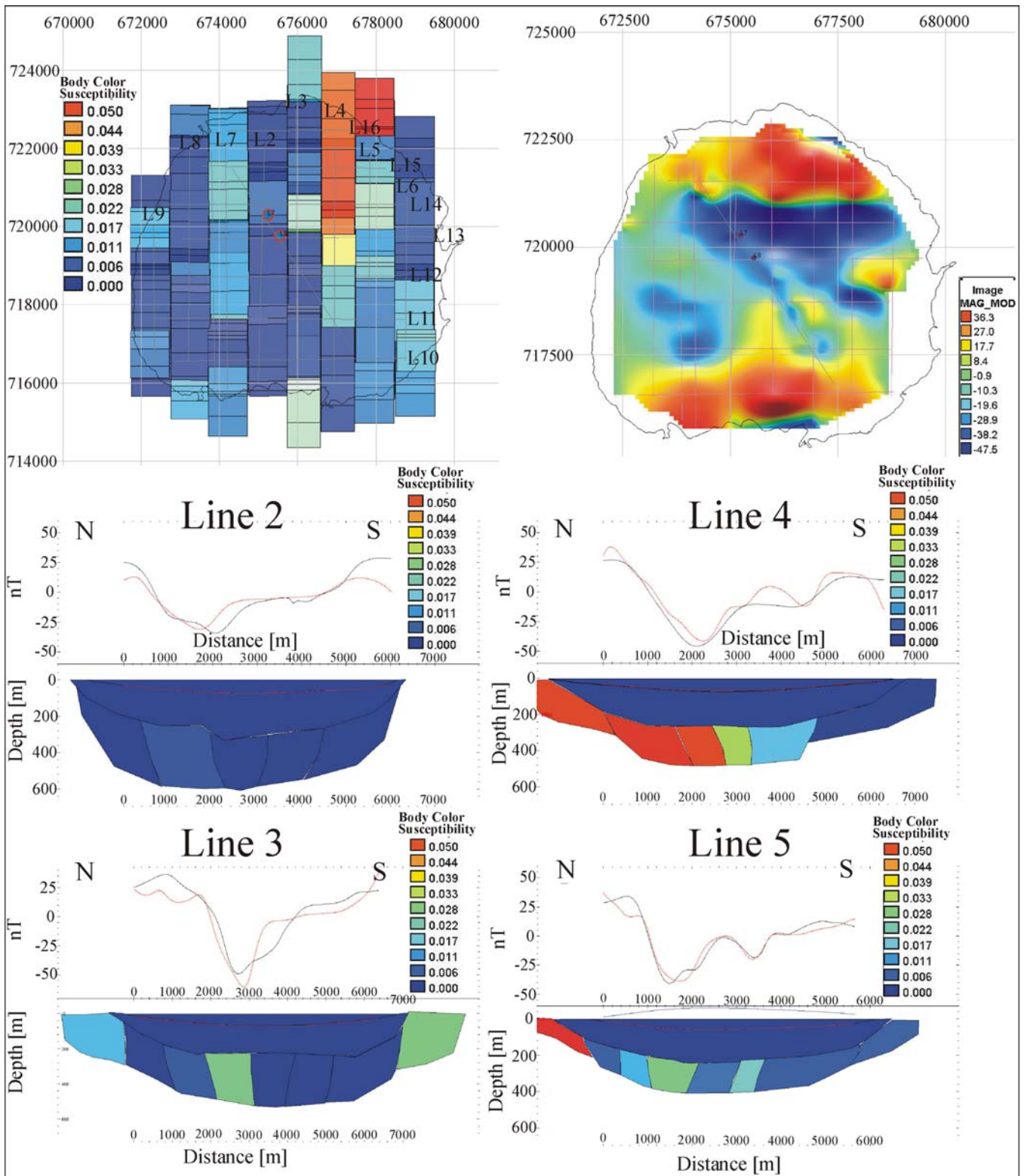


Fig. 7. Plan view and cross sections of the new 3-D model generated in this work. Top left: plan view of the magnetized bodies, color-coded by magnetic susceptibility. Top right: computed magnetic response of the 3-D model. Middle and bottom rows: four north-south cross sections of the model, from west (line 2) to east (line 5). The bodies are color-coded by magnetic susceptibility. The body at the top is water ($k = 0$), constrained by the lake bathymetry, followed by the post-impact sediment layer ($k = 0$), which is constrained by the gravity model.

et al. 2007). NRM intensities are higher than 1 A/m across most of the lake. However, as the direction of remanence is parallel to the ambient field, the real effect of increasing the intensity of NRM is to increase the effective susceptibility,

$$k_{eff} = k(1 + Q) = k \left(1 + \frac{\|\overline{M}_R\|}{\|\overline{M}_I\|} \right) \quad (1)$$

where k is magnetic susceptibility, k_{eff} is the effective susceptibility after adding remanence, Q the Koeningberger ratio, and M_I and M_R are the intensity of the induced and remanent magnetization, respectively. Consequently, the same effect can be accomplished by reducing the intensity of NRM and increasing susceptibility or vice-versa, but reasonable limits on the amount of each are imposed by magnetic mineralogy (compare Kontny et al. 2007).

Analysis of the amplitude of the analytical signal map (Fig. 4) also locates the main source of the observed magnetic anomaly at the northeast corner of the lake (A1, A2 of Fig. 4), and on a northeast to southwest line to the south of it (B1 and B2 of Fig. 4), which—not surprisingly—aligns with the highest magnetic susceptibilities found by the model.

DISCUSSION

We succeeded in finding a model that fits the observed magnetic anomalies and the petrophysical measurements from the ICDP boreholes LB-07A and LB-08A. However, there are still some unresolved problems that we attempt to address here. Due to the expected relatively high magnetization of impact-melt rocks (Ugalde et al. 2005; Henkel and Reimold 2002), the amount of impact melt produced by the Bosumtwi impact becomes an important constraint in understanding the source of the observed magnetic anomalies. Artemieva et al. (2004) estimated the volume of impact melt produced by the impact (projectile diameter between 0.76–1.04 km for an impact angle between 30°–60°, impacting at 20 km/s) at 2.6–4.3 km³, and a thickness of ~200 m for the melt sheet near the location of the two ICDP deep boreholes. Plado et al. (2000) interpreted the observed magnetic anomalies as an approximately triangular body of impact melt extending for 4000 m in the north-south direction, of 400 m thickness, and of 4000 m width in east-west extent, which would give approximately 3.2 km³ of impact melt. However, the ICDP deep boreholes did not find a considerable amount of impact melt, just centimeter-wide suevite dikes in LB-08A and <50 m of suevite in LB-07A (Coney et al. 2007; Ferrière et al. 2007; Deutsch et al. 2007). In addition, the melt proportion in suevitic breccias in these boreholes was shown by these authors to be generally very small, amounting to just a few volume %. The gravity model of Ugalde et al. (2007) also supports an impactite unit much thinner than expected. Therefore, there are three options to understand the source of the magnetic anomalies: a) the ICDP

deep boreholes missed the true source of the magnetic anomalies, and there is a large body of magnetic rock below the ICDP boreholes, but at a greater depth; b) there is a large body of impact melt in the northeast sector of the impact structure; c) the source of the magnetic anomalies is not impact melt, and another source mechanism has yet to be found.

The first option can be ruled out based on the magnetic properties of the impactites measured around the lake by Plado et al. (2000), and the magnetic properties of the target lithologies measured by Kontny et al. (2007). Because of the exponential decay of the magnetic anomalies with depth to the top of the associated magnetic sources (Spector and Grant 1970), in order to have a deeper magnetic source below the ICDP deep boreholes, the magnetic properties of these bodies would have to be at least ten times those measured around the lake or at the ICDP boreholes. That is very unlikely considering the magnetic properties measured in a few melt fragments found in the impact breccia and the target lithologies at LB-07A and LB-08A (Kontny and Just 2006; Kontny et al. 2007). Kontny et al. (2007) measured an average susceptibility of $\sim 300 \times 10^{-6}$ SI and $Q \sim 9$ for the target lithologies. That would give an effective susceptibility of $k_{eff} = k(1 + Q) = 3000 \times 10^{-5}$ SI for the whole stratigraphic column, which is still not sufficient to produce such large anomalies. Also, if that were the case, the borehole magnetic logs would show much higher amplitude anomalies towards the base of the boreholes (Morris et al. 2007). Furthermore, the location of the ICDP deep boreholes does not match the location of any of the magnetic anomalies, as indicated by the amplitude of the analytical signal (Fig. 4), nor does the wavelength of the anomalies correspond to what is expected for a magnetic source located 500 m below the observation plane (much broader anomalies, highly reduced amplitudes). Plado et al. (2000) interpreted the magnetic anomalies as impact melt, based on the hypothesis that the magnetic properties of the suevites around the lake were diminished by weathering and alteration processes. Thus, the measured values were not representative of the real magnetization parameters of the impact-melt rocks that were assumed to be inside the impact structure. Kontny et al. (2007) indeed showed that the rock magnetic parameters for all rocks at the ICDP deep boreholes (impact lithologies and basement rocks) are distinctly higher than those reported by Plado et al. (2000); however, neither ICDP deep borehole intersected any impact melt (Coney et al. 2007; Ferrière et al. 2007; Deutsch et al. 2007), which rules out impact melt as a magnetic source. Finally, based on the location of the magnetic anomalies, and their wavelength and intensity, we cannot locate the source of the magnetic anomalies below the ICDP deep boreholes, at a greater depth.

The second and third options have similar implications regarding the location of the magnetic sources, but differ with regard to the origin of the anomalies. Considering both the

3-D model constructed here and the amplitude of the analytical signal map (Figs. 4 and 7), the magnetic sources are located to the northeast of the lake. However, the genesis of these magnetic anomalies has yet to be explained. The impact-melt alternative as a source of the northeast magnetic anomalies is difficult to conceive because of a) the low magnetic properties of the impact melt found in LB-08A and LB-07A, and b) the expected symmetry of a crater structure such as this one. Slumping and/or movement of basement mega-blocks that could have removed the expected impact melt from the LB-08A and LB-07A area is an option, in comparison with the observations at the Chicxulub ICDP borehole YAX-1 (Dressler et al. 2003); however the marine magnetic data do not show any evidence of faulting that would support this hypothesis. The numerical modeling by Artemieva (2004) suggested that the impactor came from the northeast at an angle of 30–45°. In this scenario, it is expected to find a higher degree of deformation in the northeast sector of the crater structure. Therefore, the magnetic anomalies on this side of the crater (A1–A3) could also represent strongly deformed areas where the temperatures were sufficiently high to effect pyrrhotite remagnetization (Kontny et al. 2007). However, this idea relies on larger amounts of vol% pyrrhotite in these rocks, whereas the observed abundance of this mineral is far less than 1 vol% in the samples from the ICDP boreholes (W. U. Reimold, personal communication), to the southwest of these anomalies. Finally, by superimposing the geology of the lake surroundings (Koeberl and Reimold 2005) and the airborne magnetic data set (Pesonen et al. 2003), there is a clear relation between the intrusives of the Kumasi batholith (KB) and the magnetic anomalies observed to the northeast of the crater, and possibly to the southwest as well, although intrusives have not been mapped in that area. Figure 8 shows a composite map of the amplitude of the analytical signal from the airborne magnetic data set (Pesonen et al. 2003) and the mapped geology (Koeberl and Reimold 2005). For simplicity, the main magnetic trends were marked with dotted lines, and the main magnetic anomalies were numbered. The magnetic anomalies to the northeast of the crater (1 of Fig. 8) are located in a NE-SW trend that is parallel to two outcrops of KB, to the northeast of the trend. Anomalies 2 and 3 are located on another NE-SW trend to the south of the previous one, but as there are no outcrops of KB to the southwest of the crater, their magnetic source is uncertain. They could be related to the Bansu Intrusion (BI), outcropping to the east and west (like anomaly 4, located on a NE-SW trend that starts at the BI outcrop on the lake shore), or to an unmapped or not-outcropping occurrence of granitoid. Anomaly 5 is located just above an occurrence of BI, so we interpret this as the magnetic source. Anomaly 6 corresponds to two sets of anomalies on another NE-SW trend in between two KB outcrops, so we interpret them as extensions of KB toward the southwest. Anomaly 7 is located in between KB outcrops;

that plus the similar frequency content and intensity of the anomalies to those of anomaly 6, allow us to interpret anomaly 7 as KB. Anomalies 8, 9, and 10 are located on the edge of the metavolcanic belt of the Birimian Supergroup (Mv of Fig. 2); their similar intensity to anomaly 11 (widespread anomaly located on top of Mv), and smaller intensity than anomalies 3, 6, 7 (associated to KB) permit us to interpret them as Mv as well.

Therefore, the main magnetic anomalies within the lake region (1 and 2 of Fig. 8) can be interpreted without any “highly magnetic impact melt,” as demanded by previous workers (Danuor 2004; Plado et al. 2000). This hypothesis is supported by a forward model carried out on the total magnetic intensity (TMI) data for borehole LB-08A by Morris et al. (2007). The borehole TMI data can be replicated by placing a prismatic magnetic source body of $3000 \times 3000 \times 3000$ m, top at 300 m depth, strike = 40°, dip = 15°, $k = 0.2$ SI, to the northwest of borehole LB-08A. With a vertical borehole and an inclined source contact the observed sharp magnetic boundary is replicated by the borehole passing through an edge of the source body (Morris et al. 2007).

By putting together the amplitude of the analytical signal from the marine data set (Fig. 4) and the geology of the lake (Koeberl and Reimold 2005), the relationship between the main anomalies (A1, A2, A3) and the Kumasi batholith intrusives is even more evident (Fig. 9). The anomalies south of B1 and B2 might be related to olivine pyroxenite, dolerite, and gabbro, which were mapped as minor intrusives at the eastern side of the Bosumtwi structure (Koeberl and Reimold 2005, and references therein) (OI of Fig. 9). The anomalies C2 and B3 exhibit weaker amplitudes than B1 and B2, probably related to a deeper location of the intrusives, assuming that they represent a continuation of the Kumasi batholith that outcrops to the north, or different and minor magnetic properties, if these anomalies are really caused by the granodiorites of the Bansu intrusion, which outcrops in a wide area to the southwest of the lake, and on its shore at Bansu (Koeberl and Reimold 2005).

Kontny et al. (2007) performed rock magnetic and magnetic mineralogy analysis on rock samples from LB-07A and LB-08A that established ferrimagnetic pyrrhotite as the main magnetic carrier for both target and impact lithologies at Bosumtwi. Shock-induced remagnetization of the pre-impact pyrrhotite was presented as a mechanism to enhance the magnetization parameters of target and impact lithologies from the values measured on material from the environs of the impact structure (Plado et al. 2000) to the values required by magnetic modeling by Plado et al. (2000) and this work. This mechanism is feasible considering the low Curie temperature of pyrrhotite (~320° C). However, pyrrhotite also demagnetizes when subject to modest shock pressures ($P < 4$ GPa) (Louzada et al. 2005). Thus for this mechanism to be effective, the area of thermal-remagnetization would have to be larger than the area of shock-demagnetization. In any case,

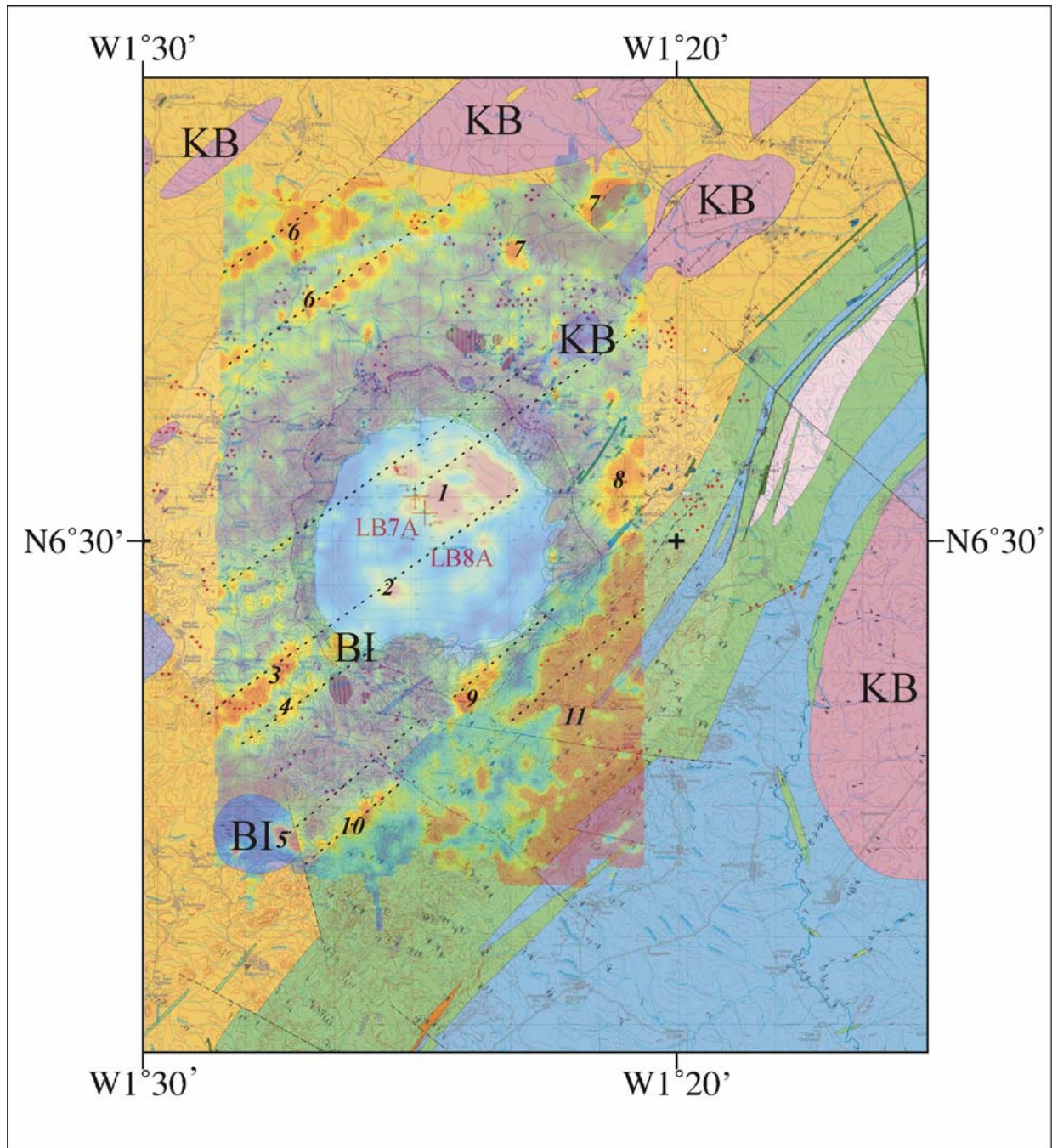


Fig. 8. Amplitude of the analytical signal from the airborne magnetic data set superimposed onto the regional geology around the Bosumtwi impact structure. The granitoids of the Kumasi batholith are marked KB; biotite and hornblende granodiorites of the Bansu intrusion are marked BI. The main trends in the magnetic data are marked as dotted lines, and the main magnetic anomalies are numbered for easier identification. See text for details.

the Q -values measured by Kontny et al. (2007) are much higher than 1, indicating that remanent magnetization dominates over induced magnetization, which could also explain why the magnetic susceptibility logs on LB-08A and LB-07A do not show values as high as the magnetic models require. Considering the age of the structure, the remanent magnetization vector has to be subparallel to the inducing

field, therefore higher Q -values translate into really high effective susceptibilities. However, if pyrrhotite was the source of the observed marine and airborne magnetic anomalies, then consistent magnetic anomalies would be observed in the borehole magnetic logs from LB-08A. Morris et al. (2007) did not find any significant magnetic anomalies on the borehole magnetic data, and furthermore explain the

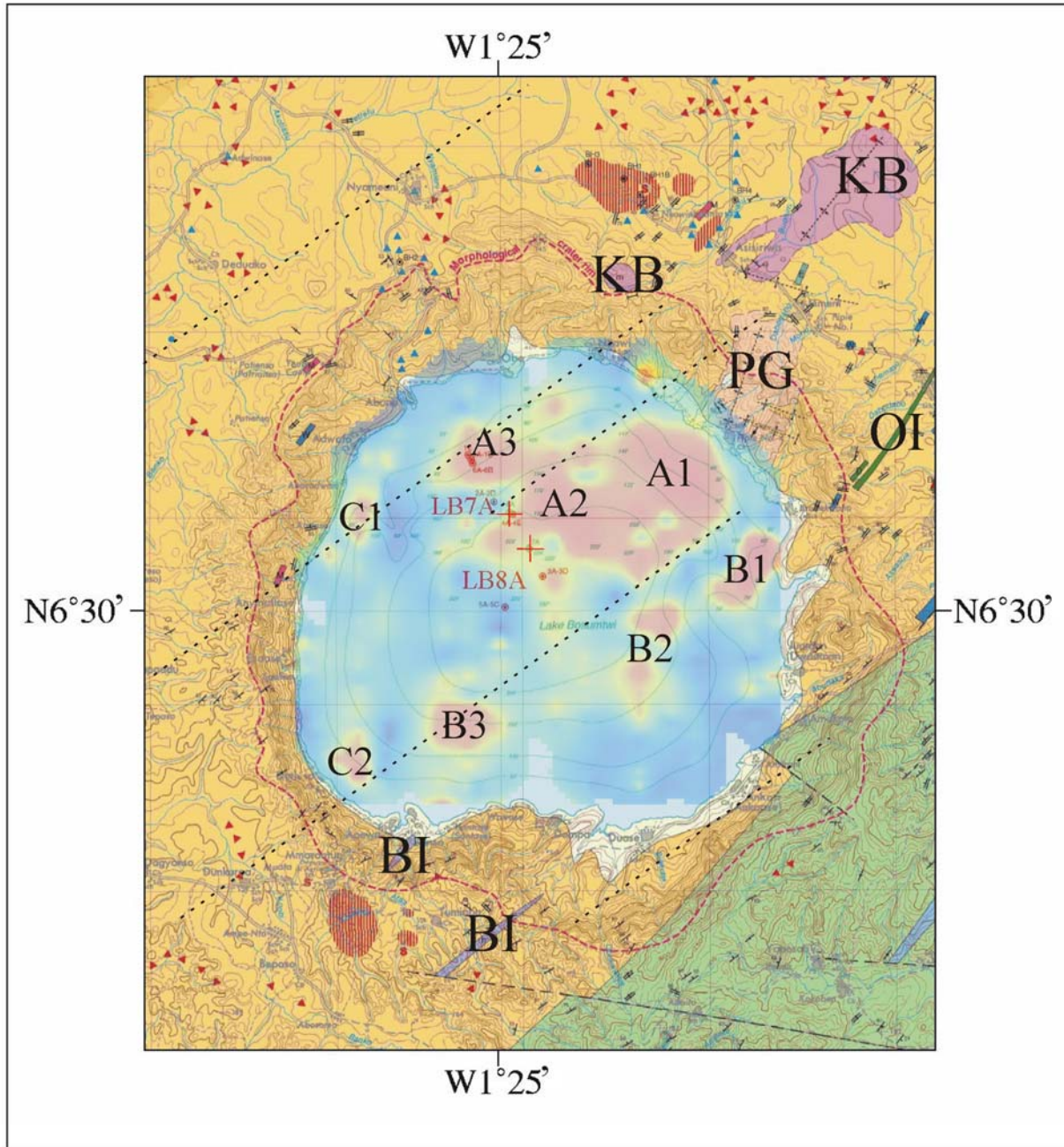


Fig. 9. The amplitude of the analytical signal from the marine magnetic superimposed onto the geology on the environs of the Bosumtwi impact crater. KB = granitoids of the Kumasi batholith; BI = biotite and hornblende granodiorites of the Bansu intrusion; PG = Pepiakese granite and diorite; OI = olivine pyroxenite, dolerite, and gabbro. The magnetic anomalies interpreted on Fig. 4 are marked A1–A3, B1–B3, and C1–C2. The ICDP deep borehole sites are marked by red crosses. The main magnetic trends interpreted from the airborne magnetic data set are marked as dotted lines. See text for details.

observed anomalies with a model consisting of one magnetized body towards the northeast of the lake and that barely intersects LB-08A at ~300 m depth, to continue as an off-hole source downwards.

Consequently, to obtain a definite explanation for the source of the observed magnetic anomalies in the northeastern sector of the crater, more information is required

on the magnetic mineralogy and properties of the rocks occurring to the northeast of the lake, and on the Kumasi batholith and Bansu intrusion located to the northeast and southwest of the lake, respectively.

Meteorite impacts can greatly modify the magnetic properties of the target rocks (Ugalde et al. 2005; Henkel and Reimold 2002), either enhancing them (e.g., higher magnetic

susceptibility because of shock decomposition of original minerals into more magnetic phases, like the shock decomposition of biotite into magnetite at 40 GPa [Chao 1968]; increase of NRM by adding a secondary component, like shock remanent magnetization [SRM] at 30 GPa [Halls 1979]; increase of NRM by melting and subsequent cooling under the presence of a magnetic field), or reducing them (e.g., magnetic susceptibility reduction at $P < 10$ GPa [Pilkington and Grieve 1992]; shock demagnetization at $P < 1$ GPa [Cisowski and Fuller 1978]). In the case of Lake Bosumtwi, the maximum shock pressures induced by the impact apparently did not reach the high values predicted by numerical modeling (Artemieva et al. 2004), and indeed reached maximum values of $P < 29$ GPa in the ICDP borehole region (Deutsch 2006). Considering the spherical propagation of the shock wave, its decay as r^{-3} , and the location of the ICDP boreholes relative to the impact structure (near center), the maximum shock pressures reached by the impact should not be higher than that measured in the ICDP borehole region. Indeed, analysis of shock metamorphism on samples from the granitoids of the Papiakese body at the northeast of the lake showed only minor fracturing of possible shock origin and shock pressure was estimated as $P < 8$ GPa (W. U. Reimold, personal communication). In all likelihood the magnetic properties of the intrusives that are the source of the observed magnetic anomalies did not change significantly, except for the remagnetization of the pre-impact formed pyrrhotite (Kontny et al. 2007), which however occurs in volumes that are not sufficiently large (mostly below 1% vol.; Kontny et al. 2007; W. U. Reimold, personal communication) to have a noticeable effect on the measured total field, either from marine, airborne, or borehole platforms. Consequently, and as can be observed on the amplitude of the analytic signal from the airborne total field on Fig. 8, the magnetization patterns observed on a macroscopic scale (airborne, marine, borehole) are similar inside and outside the crater.

This rejects Plado et al.'s (2000) hypothesis about the Papiakese granite (PG of Fig. 9) as a probable indicator of the availability of biotite-rich rocks that could have decomposed into magnetite due to the impact. However, the Papiakese granitoid also contains a dioritic phase (W. U. Reimold, personal communication), which could have higher magnetic properties than what was measured by Plado et al. (2000) on its granitic phase, and that is not sufficiently high to generate the observed magnetic anomalies to the northwest and southeast of the lake.

CONCLUSIONS

Synthetic magnetic profiles of a body at equatorial latitudes were helpful in showing that the magnetic anomalies at low magnetic latitudes show distinct features which help in locating the source body. In plan view they show the central negative anomaly with asymmetric northern and southern

flank anomalies. The amplitude of the analytic signal was valuable in locating the source of the observed magnetic anomalies.

Based on the high-resolution marine magnetic data acquired at Lake Bosumtwi, a new 3-D magnetic model was constructed for the Bosumtwi structure. The model has the same geometry as a 3-D gravity model of the structure, and it is consistent with previous seismic models and the petrophysical data from cores obtained from the ICDP deep holes LB-07A and LB-08A. The model consists of a stack of 3-D bodies with moderate magnetic properties across the lake, but highly magnetic bodies located to the northeast of the lake are the most significant feature. Integration of the new 3-D model, the newly published geological map of the structure, the ICDP borehole petrophysics and geology, and the airborne and marine magnetic data sets allowed to interpret the observed magnetic anomalies based on the mapped geology. The magnetic anomalies on the lake are likely caused by granodiorites of the Kumasi batholith, or granodiorites of the Papiakese intrusion. There is no need for highly magnetic melt volumes, which were not confirmed through the ICDP boreholes. In order to verify this, detailed magnetic scanning of the Kumasi and Bansu intrusions is required.

Acknowledgments—Drilling at Bosumtwi was supported by the International Continental Scientific Drilling Program (ICDP), the U.S. NSF-Earth System History Program under grant no. ATM-0402010, Austrian FWF (project P17194-N10), the Austrian Academy of Sciences, and by the Canadian Natural Sciences and Engineering Research Council (NSERC). Drilling operations were performed by DOSECC. Local help by the Geological Survey Department (Accra) and the Kwame Nkrumah University of Science and Technology (KNUST, Kumasi), Ghana, were invaluable. We thank the associate editor W. U. Reimold and A. Kontny for helpful comments and suggestions that really improved the manuscript.

Editorial Handling—Dr. Wolf Uwe Reimold

REFERENCES

- Artemieva N., Karp T., and Milkereit B. 2004. Investigating the Lake Bosumtwi impact structure: Insight from numerical modeling. *Geochemistry Geophysics Geosystems* 5:1–20.
- Boamah D. and Koeberl C. 2003. Geology and geochemistry of shallow drill cores from the Bosumtwi impact structure, Ghana. *Meteoritics & Planetary Science* 38:1137–1159.
- Chao E. C. T. 1968. Pressure and temperature histories of impact metamorphosed rocks—Based on petrographic observations. In *Shock metamorphism of natural materials*, edited by B. M. French and N. M. Short. Baltimore: Mono Book Corp. pp.135–158.
- Cisowski S. M. and Fuller M. 1978. The effect of shock on the magnetism of terrestrial rocks. *Journal of Geophysical Research* 83:3441–3458.

- Coney L., Gibson R. L., Reimold W. U., and Koeberl C. 2007. Lithostratigraphic and petrographic analysis of ICDP drill core LB-07A, Bosumtwi impact structure, Ghana. *Meteoritics & Planetary Science* 42. This issue.
- Danuor S. K. 2004. Geophysical investigations of the Bosumtwi impact crater and comparison with terrestrial meteorite craters of similar age and size. Ph.D. thesis, Kwame Nkrumah University of Science and Technology, Kumasi, Ghana.
- Deutsch A. 2006. Lake Bosumtwi drilling project: Shock metamorphism in rocks from core BCDP-8A vs. experimental data (abstract #1327). 37th Lunar and Planetary Science Conference. CD-ROM.
- Deutsch A., Luetke S., and Heinrich V. 2007. The ICDP Lake Bosumtwi impact crater scientific drilling project (Ghana): Core LB-08A litho-log, related ejecta, and shock recovery experiments. *Meteoritics & Planetary Science* 42. This issue.
- Dressler B. O., Sharpton V. L., Morgan J., Buffler R., Moran D., Smit J., Stoeffler D., and Urrutia-Fucugauchi J. 2003. Investigating a 65 Ma old smoking gun: Deep drilling of the Chicxulub impact structure. *Eos Transactions* 84:125–130.
- Elbra T., Kontny A., Pesonen L. J., Schleifer N., and Schell C. 2007. Petrophysical and paleomagnetic data of drill cores from the Bosumtwi impact structure, Ghana. *Meteoritics & Planetary Science* 42. This issue.
- Ferrière L., Koeberl C., and Reimold W. U. 2007. Drill core LB-08A, Bosumtwi impact structure, Ghana: Petrographic and shock metamorphic studies of material from the central uplift. *Meteoritics & Planetary Science* 42. This issue.
- Henkel H. and Reimold W. U. 2002. Magnetic model of the central uplift of the Vredefort impact structure, South Africa. *Journal of Applied Geophysics* 51:43–62.
- Halls H. C. 1979. The Slate Islands meteorite impact site: A study of shock remanent magnetization. *Geophysical Journal of the Royal Astronomical Society* 59:553–591.
- Jones W. B., Bacon M., and Hastings D. A. 1981. The Lake Bosumtwi impact crater, Ghana. *Geological Society of America Bulletin* 92:342–349.
- Junner N. R. 1937. The geology of the Bosumtwi caldera and surrounding country. *Gold Coast Geological Survey Bulletin* 8: 1–38.
- Karp T., Milkereit B., Janle J., Danuor S. K., Pohl J., Berckhemer H., and Scholz C. A. 2002. Seismic investigation of the Lake Bosumtwi impact crater: Preliminary results. *Planetary Space Science* 50:735–743.
- Koeberl C., Bottomley R., Glass B. P., and Storzer D. 1997. Geochemistry and age of Ivory Coast tektites and microtektites. *Geochimica et Cosmochimica Acta* 61:1745–1772.
- Koeberl C. and Reimold W. U. 2005. Bosumtwi impact crater, Ghana (West Africa): An updated and revised geological map, with explanations. *Jahrbuch der Geologischen Bundesanstalt, Wien (Yearbook of the Austrian Geological Survey)* 145:31–70 (+1 map, 1:50,000).
- Koeberl C., Milkereit B., Overpeck J. T., Scholz C. A., Amoako P. Y. O., Boamah D., Danuor S., Karp T., Kueck J., Hecky R. E., King J. W., and Peck J. A. 2007. An international and multidisciplinary drilling project into a young complex impact structure: The 2004 ICDP Bosumtwi Crater Drilling Project—An overview. *Meteoritics & Planetary Science* 42. This issue.
- Kontny A. and Just J. 2006. Magnetic mineralogy and rock magnetic properties of impact breccias and crystalline basement rocks from the BCDP-drillings 7A and 8A (abstract #1343). 37th Lunar and Planetary Science Conference. CD-ROM.
- Kontny A., Elbra T., Just J., Pesonen L. J., Schleicher A. M., and Zolk J. 2007. Petrography and shock-related remagnetization of pyrrhotite in drill cores from the Bosumtwi Impact Crater Drilling Project, Ghana. *Meteoritics & Planetary Science* 42. This issue.
- Louzada K. L., Stewart S. T., and Weiss B. P. 2005. Shock demagnetization of pyrrhotite (abstract #1134). 36th Lunar and Planetary Science Conference. CD-ROM.
- MacLeod I. N., Jones K., and Dai T. F. 1993. 3-D analytic signal in the interpretation of total magnetic field data at low magnetic latitudes. *Exploration Geophysics* 24:679–688.
- Milkereit B., Ugalde H., Karp T., Scholz C. A., Schmitt D., Danuor S. K., Artemieva N., Kueck J., Qian W., and L'Heureux E. 2006. Exploring the Lake Bosumtwi crater—Geophysical surveys, predictions and drilling results (abstract #1687). 37th Lunar and Planetary Science Conference. CD-ROM.
- Moon P. A. and Mason D. 1967. The geology of 1/4° field sheets nos. 129 and 131, Bompata S.W. and N.W. *Ghana Geological Survey Bulletin* 31:1–51.
- Morris W. A., Ugalde H., and Clark C. 2007. Physical property measurements: ICDP boreholes LB-07A and LB-08A, Lake Bosumtwi impact structure, Ghana. *Meteoritics & Planetary Science* 42. This issue.
- Nabighian M. 1972. The analytic signal of two-dimensional magnetic bodies with polygonal cross-section: Its properties and use for automated anomaly interpretation. *Geophysics* 37:507–517.
- Pesonen L. J., Koeberl C., Reimold W. U., and Brandt D. 1997. New studies of the Bosumtwi impact structure, Ghana: The 1997 field season (abstract). *Meteoritics & Planetary Science* 32:A72–73.
- Pesonen L. J., Koeberl C., and Hautaniemi H. 2003. Airborne geophysical survey of the Lake Bosumtwi meteorite impact structure (southern Ghana)—Geophysical maps with descriptions. *Jahrbuch der Geologischen Bundesanstalt, Vienna (Yearbook of the Austrian Geological Survey)* 143:581–604.
- Pilkington M. and Grieve R. A. F. 1992. The geophysical signature of terrestrial impact craters. *Reviews of Geophysics* 30:161–181.
- Plado J., Pesonen L. J., Koeberl C., and Elo S. 2000. The Bosumtwi meteorite impact structure, Ghana: A magnetic model. *Meteoritics & Planetary Science* 35:723–732.
- Reimold W. U., Brandt D., and Koeberl C. 1998. Detailed structural analysis of the rim of a large, complex impact crater: Bosumtwi crater, Ghana. *Geology* 26:543–546.
- Roest W., Verhoef J., and Pilkington M. 1992. Magnetic interpretation using the 3-D analytic signal. *Geophysics* 57:116–125.
- Schleifer N. H., Elster D., and Schell C. M. 2006. Petrophysical characterization of the core samples of the Bosumtwi meteorite impact crater (Ghana) (abstract #1273). 37th Lunar and Planetary Science Conference. CD-ROM.
- Scholz C. A., Karp T., Brooks K. M., Milkereit B., Amoako P. Y. O., and Arko J. A. 2002. Pronounced central uplift identified in the Bosumtwi impact structure, Ghana, using multichannel seismic reflection data. *Geology* 30:939–942.
- Spector A. and Grant F. S. 1970. Statistical models for interpreting aeromagnetic data. *Geophysics* 35:293–302.
- Ugalde H. A., Artemieva N., and Milkereit B. 2005. Magnetization on impact structures—Constraints from numerical modeling and petrophysics. In *Large meteorite impacts III*, edited by Kenkmann T., Hörz F., and Deutsch A. GSA Special Paper #384. Boulder, Colorado: Geological Society of America. pp. 25–42.
- Ugalde H. 2006. Geophysical signature of midsize to small terrestrial impact craters. Ph.D. thesis, University of Toronto, Toronto, Ontario, Canada.
- Ugalde H., Danuor S. K., and Milkereit B. 2007. Integrated 3-D model from gravity and petrophysical data at Lake Bosumtwi, Ghana. *Meteoritics & Planetary Science* 42. This issue.